Iodine-131-Metaiodobenzylguanidine Dosimetry in Cancer Therapy: Risk Versus Benefit

Maria Tristam, Abdulaziz S. Alaamer, John S. Fleming, Valerie J. Lewington and Maureen A. Zivanovic
Department of Nuclear Medicine, Southampton General Hospital, Southampton, United Kingdom

In the treatment of neural crest tumors, such as pheochromocytoma, with [^{131}I]MIBG, bone marrow toxicity limits the amount of administered activity and, thus, a therapeutically useful tumor dose. **Methods:** We calculated tumor doses in a series of diagnostic studies with [^{123}I]MIBG using accurate quantification of SPECT and planar scintigraphy. By extrapolating diagnostic results to therapeutic activities of [^{131}I]MIBG, we could compare the results with whole-body doses from a series of therapies. **Results:** The tumor dose was $D_T = 2.2$ mGy MBq^{-1} (median value of 27 measurements, range $0.04 \leq D_T \leq 20$ mGy MBq^{-1}) and the whole-body dose in a series of 16 patients undergoing 50 therapies was $D_{WB} = 0.12 \pm 0.04$ mGy MBq^{-1} (mean ± s.d.). The therapeutic ratio varied between 130 to below 10 in some patients. **Conclusion:** The results were compared with published data. We found clearly skewed distribution of tumor doses, with a majority of tumors receiving only a few mGy per MBq administered activity. In some patients, however, doses did reach 20 mGy MBq^{-1}.

Key Words: iodine-123-MIBG; pheochromocytoma; radionuclide therapy; dosimetry

J Nucl Med 1996; 37:1058–1063

In cancer therapy with systemically administered radiopharmaceuticals, such as ^{131}I-labeled metaiodobenzylguanidine (MIBG) used in the treatment of neural crest tumors, the benefit must be balanced against possible complications. The aim of the treatment is to sterilize cancer cells. Therefore, the absorbed radiation dose to the tumor is a useful measure of the efficacy of the treatment. The most frequent side effect is thrombocytopenia (*1*). Thus, the dose to the bone marrow is a measure of toxicity (although a recent hypothesis (*2*) suggests that thrombocytopenia is not only dependent on the overall bone marrow dose but is caused by specific uptake and subsequent damage to the precursor cells of the platelets).

Ideally, one would like to have tumor and bone marrow dose data for a specific patient prior to a planned MIBG therapy and prescribe the amount of administered activity accordingly. This, however, is far from easy. The true dose to the bone marrow is difficult to estimate because of the complex distribution of hemopoietic tissue in the body. In practice, the absorbed whole-body dose is used as an adequate representation or index of bone marrow toxicity. To measure the whole-body dose prior to therapy, one must measure retention of a tracer dose of MIBG using a whole-body counter or a probe held at a constant and sufficiently large distance. Iodine-131-MIBG is most suitable for this purpose, since ^{123}I is too short-lived (13-hr half-life as opposed to 193 hr) to measure the multiexponential pattern of whole-body clearance. On the other hand, [^{123}I]MIBG is most suitable for tumor dosimetry: best estimates of tumor dose are obtained from accurate quantification of sequential scintigraphic images and ^{123}I possesses more superior imaging properties (with photopeak energy of 159 keV) than ^{131}I (364 keV).

Thus, an ideal scenario for a pretreatment investigation would include both ^{123}I tumor dosimetry and ^{131}I whole-body dosimetry (assuming that differences in specific activity and concentration of diagnostic and therapeutic MIBG do not preclude extrapolation of results from diagnosis to treatment). To undergo such complex investigations would be exhausting for the patients and also prohibitively expensive. As an alternative, other predictors of toxicity have been proposed, such as activity adjusted to body weight or body area (*1*). Doses to other critical organs have also been calculated (*3*), but the tolerance levels of organs such as liver and lungs, which became irradiated in the course of MIBG treatment, are much higher than that of bone marrow (*4*). The issue of radiation tolerance levels of various organs and tissues is complex: values derived from external beam radiotherapy and fractionated schedules ignore the possible effects of a low dose rate, which is an important consideration in targeted radiotherapy (*5*).

Although pretherapy estimates of whole-body doses are difficult, this can be readily calculated from post-therapy retention measurements. In this study, we compared tumor dosimetry from diagnostic tracer imaging with whole-body doses calculated from post-therapy measurements.

MATERIALS AND METHODS

Diagnostic Series

Thirteen patients with confirmed pheochromocytoma were investigated. Twenty quantifiable lesions were detected and, since some patients had more than one study, 27 independent measurements were obtained and analyzed.

The standard imaging protocol was as follows: patients were injected with 370 MBq (10 mCi) [^{123}I]MIBG (74 MBq ml^{-1}, specific activity 148 MBq mg^{-1}). After the injection, planar gamma camera images were obtained at 5 min, 2 hr, and then 6, 24, 30 and 48 hr. This enabled estimation of the effective half-life of MIBG in the tumor. At the time of 24-hr imaging, a SPECT study was also acquired. Tumor activity and volume were calculated directly from SPECT and the time-activity curve re-calibrated in absolute units of activity versus time, which enabled calculation of the half-life of MIBG in tumor.

SPECT quantification played a crucial role in this study. A method of analysis, utilizing a technique of threshold determination known as maximization of interclass variance, was used (*6*). The technique was evaluated extensively in a series of phantom measurements (*7*) that studied the effect of various object-related and surrounding-related factors on its accuracy and precision. The

Received May 19, 1995; revision accepted Sept. 21, 1995.
For correspondence or reprints contact: Maria Tristam, MD, Nuclear Medicine, Southampton General Hospital, Level D, Centre Block, Tremona Rd., Southampton SO16 6YD, United Kingdom.

SPECT reconstruction algorithm incorporated corrections for both scattered radiation and attenuation. The map of the attenuation co-efficient used for the latter correction was obtained either from aligned CT data (*8*) or standard outline images (*9*). The method was shown to be accurate and reproducible, if a consistent regimen was used in its application. This method is superior to alternative estimates of tumor volume from CT or MR scans. Although the resolution of both CT and MR is much better, only the anatomical extent of the tumor mass can be obtained from these imaging methods. SPECT, however, yields the required functional volume.

Therapeutic Series

Sixteen patients, twelve adults and one 14-yr-old child with pheochromocytoma and four children, aged 5–8 yr, with neuroblastoma, were treated with a standard therapeutic activity of 7.4 GBq (200 mCi) [^{131}I]MIBG (37 MBq ml^{-1}, specific activity 1–2 GBq mg^{-1}), in 50 treatments. The activity was administered over 45–100 min to avoid precipitation of a catecholamine crisis (*10*). Whole-body doses were calculated from post-therapy retention measurements. These measurements were obtained using a Geiger-Muller probe positioned at a constant distance (2–5 m) from the patient's bed. Such measurements, if performed with sufficient frequency, especially during the initial fast phase, provide reproducible results.

The two patient groups did not consist of the same individuals. On occasion, patients were treated without formal pretreatment image quantification because tumor spread was so extensive and/or irregular that accurate quantification was not possible. Conversely, the results of the quantitative diagnostic investigation indicated that MIBG treatment in some patients was inappropriate. Thus, direct comparison of tumor and whole-body doses was possible in only 10 patients.

RESULTS

Diagnostic Series

Tumor doses calculated in diagnostic investigations performed with tracer [^{123}I]MIBG were used to predict doses following therapeutic activities of [^{131}I]MIBG, with appropriate corrections for different physical decay. Although there is controversy whether such extrapolation is entirely justified (*11*), we assumed similar biokinetics, independent of the activity of MIBG, in keeping with other authors (*11,12*) who used ^{123}I in scintigraphic studies. Consequences that might result from such a treatment are further discussed.

From analysis of sequential planar images, the effective half-life of MIBG in the tumor was found. We used experimental values of tumor activity A_T and volume V_T to calculate tumor uptake as $U = A_T/V_T$. We assumed instantaneous uptake of MIBG in the tumor, ignoring the initial upsloping phase of the time-activity curve, which is short with respect to the clearance portion of the curve. The experimental time-activity curve was extrapolated to the time of injection to obtain maximum specific uptake U_0. This extrapolated value is a little higher than the actual maximum uptake in tumor, which occurs on average at 12 hr after injection. Ignoring this portion of the time-activity curve results in a small overestimate of tumor dose of about 3% (*13*).

The values of effective half-life and specific uptake for all measurements are plotted in Figure 1. The values of specific uptake varied over tenfold between lesions studied ($0.01 \leq U_0 \leq 0.11$%/milliliter volume) with a median value of 0.038. The effective half-life values also varied considerably ($19 \leq T_{eff} \leq 100$ hr; median value 34 hr). The majority of measurements were clustered closely in the $T_{eff} - U_0$ space; two data points, corresponding to two lesions in a particular patient, were characterized by much higher uptake and a much longer retention time than the rest.

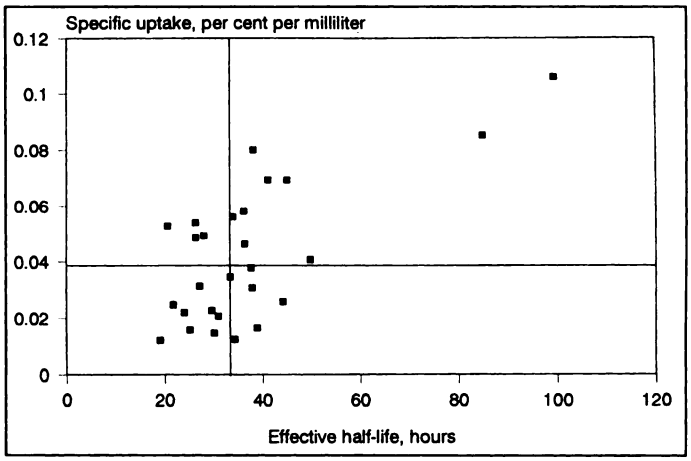

FIGURE 1. Tumor uptake versus effective half-life.

We used the median values $U_0 = 0.038$%/ml of tumor and $T_{eff} = 34$ hr (assuming a single exponential clearance curve), and determined the tumor dose using the MIRD formula:

$$D_T = A_c \times S_1,$$

where A_c is the cumulated activity, $A_c = 1.44 \times A_0 \times U_0 \times T_{eff}$, S is the mean dose per unit cumulated activity and A_0 is the administered activity in MBq. For a tumor volume of 1 ml, the S value, considering nonpenetrating radiation only and assuming tumor density of 1 gcm^{-3}, is S = 0.1105 Gy MBq^{-1}hr^{-1} (*14*). Assuming $A_0 = 1$ MBq, would result in the tumor dose $D_T = 2.0$ mGy MBq^{-1}. This result is acceptable for small tumors, but for larger tumor volumes, the S value should include the penetrating radiation contribution, which increases from about 5% at 10 ml, to about 10% at 100 ml and 25% at 1000 ml. This can be verified by comparing the S value calculated as S = 0.1105/m Gy MBq^{-1}hr^{-1}g, where m is the mass of tumor in grams, with the values tabulated for organs of different sizes and including the gamma contribution (*15*). Similar results would be obtained from the formula quoted by Hoefnagel (*16*):

$$D_\beta(\text{Gy}) = 19.9 \times C \times E \times T_{eff},$$

where C is the concentration of MIBG in MBq/g tissue, E is the average beta energy in MeV (E = 0.1916 MeV for the main beta emission of ^{131}I) and T_{eff} is in days, or Fielding et al. (*17*):

$$D_T(\text{Gy}) = 1/m \times A_c \times 1.062 \times 10^{-4},$$

where m is the tumor mass in kilograms and A_c is the cumulated activity in MBq. Both formulae include only nonpenetrating radiation contribution.

The tumor size affects the S value for larger as well as smaller tumors: for sizes of the order of beta particle ranges (i.e., the micrometastases of submillimeter dimensions), the S value must reflect the fact that the absorbed fraction is less than 1 (*18*). In general, the effect of tumor size on tumor dose and curability differs in targeted therapy and in external beam radiotherapy. Although in both situations larger tumors are more difficult to eradicate because of the greater number of clonogenic cells, microscopic tumor foci are also relatively radioresistant to targeted radionuclide treatment. This is because, as the tumor size decreases below the mean range of the emitted particles, the absorbed fraction of energy, and thus the dose, falls (*19*). For ^{131}I, the tumor size of optimal curability corresponds to micrometastases of about 3 mm diameter (*20*).

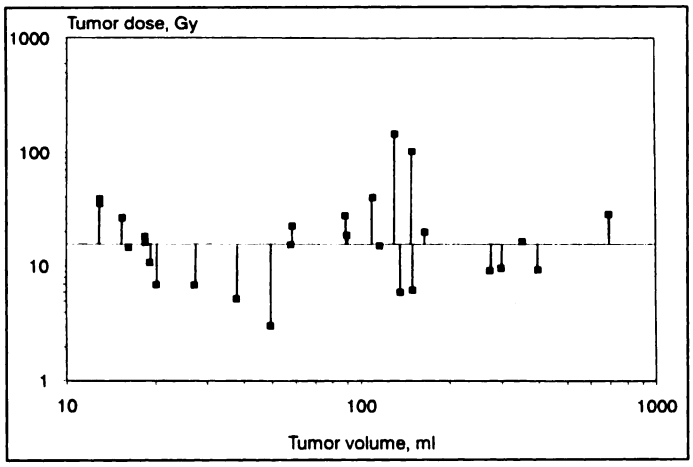

FIGURE 2. Tumor dose versus tumor volume.

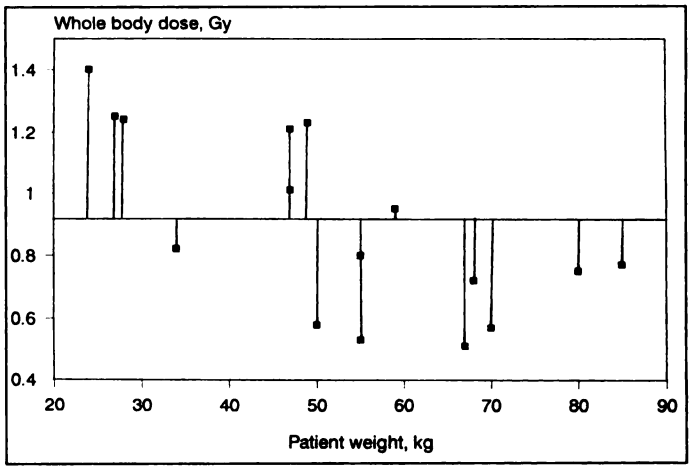

FIGURE 3. Whole-body dose versus whole-body weight.

The use of [^{131}I]MIBG in conjunction with external radiation (total-body irradiation for smaller micrometastases and single tumor cells, with high-dose localized radiotherapy for macroscopic, clinically detectable deposits), effective outside the optimal size range of the targeted radionuclide, might overcome this limitation (*21*).

In the present study, we investigated tumor volumes ranging from 13 to 700 ml. Individual tumor doses were calculated with the correction for penetrating radiation. The doses predicted following therapeutic activity of 7.4 GBq varied between 3 and 150 Gy, with the median value of 16 Gy, or D_T = 2.2 mGy MBq^{-1} (range 0.04 ≤ D_T ≤ 20 mGy MBq^{-1}), a value only slightly higher than that obtained using constant S value and neglecting the effect of penetrating radiation. In Figure 2, calculated tumor doses are plotted against tumor volume.

Therapeutic Series

Whole-body doses were calculated from post-therapy retention measurements. The measured patterns of MIBG clearance were multiexponential, with at least two exponents observed in all patients. About 10% to 15% of the administered activity is excreted with urine at the first micturation, followed by a fast clearance phase characterized by a mean half-life T_1 = 13 ± 5 hr. Subsequently, the clearance slows down to a half-life T_2 = 29 ± 6 hr. Patients are normally discharged 3–5 days after treatment and retention measurements are usually not available after that time. When they do exist (e.g., patients attending for post-therapy imaging), there is a suggestion that the clearance slows down even further. This late change in the slope of the retention curve can be ignored since over 50% of the injected activity is excreted in urine during the first day, over 75% the second and over 90%, the third day after therapy. These figures are in agreement with recently published values (*22*). The values of clearance parameters measured in the therapy series are summarized in Table 1.

In general, due to difficulties in reproducing the geometry exactly, retention measurements are not very accurate and fitting straight lines to data on semi-log graphs is prone to errors; lack of data during night periods further worsens the situation. Typically, measurement errors of a few percent, from the fitted clearance pattern, were observed, e.g., 8.8% ± 5.3% (mean ± s.d., n = 16) in one series, 5.4% ± 4.3% (mean ± s.d., n = 24) in another, etc. Measurements with large errors, which were clearly due to incorrect positioning, were rejected as outliers.

TABLE 1
Parameters of Clearance Kinetics in the Therapy Group

		Neuroblastoma	Pheochromocytoma	All patients
T_1	Mean	9 ± 2 hr	13 ± 5 hr	12 ± 5 hr
	Variation	$7 \le T_1 \le 12$	$7 \le T_1 \le 24$	$7 \le T_1 \le 24$
T_2	Mean	25 ± 3 hr	30 ± 6 hr	29 ± 6 hr
	Variation	$21 \le T_2 \le 27$	$20 \le T_2 \le 38$	$21 \le T_2 \le 38$

If the tumor burden and/or tumor function does not change significantly from one therapy to the next, the pattern of clearance remains constant for a given patient. In those cases, calculation of the whole-body dose can be made more accurate by averaging data over several therapies.

As seen in Table 1, the mean half-lives for neuroblastoma patients are slightly lower but, since patients in this subgroup were children, it is not clear whether this is due to the differences in tumor physiology, age and weight of these patients or tumor burden. These values are closely comparable with the results in the USCCSG study (Fielding, *personal communication,* 1989), 8 and 27 hr for the first and second component, respectively. In that trial, third (45 hr) and fourth (110 hr) components were measured.

Whole-body doses for each patient were calculated using the MIRD formula and the values of T_1 and T_2 were derived from retention measurements. The mean dose per unit cumulated activity:

$$S = 2.7 \times 10^{-3} \text{mGyMBq}^{-1}\text{hr}^{-1}$$

for a 70-kg "standard man" (*15*), was adjusted proportionally to body weight. Whole-body doses, for the therapeutic activity of 7.4 GBq, are plotted against body weight in Figure 3, together with the mean value for all 16 patients:

$$D_{WB} = 0.90 \pm 0.29\text{Gy},$$

which corresponds to 0.12 ± 0.04 mGy per MBq administered activity (mean ± s.d.). Analysis of this graph suggests a slight correlation between the whole-body absorbed dose and body weight: the mean in the neuroblastoma children group was 0.16 mGY MBq^{-1}; the mean in pheochromocytoma group was 0.12 mGY MBq^{-1}.

The clearance kinetics and the whole-body dose depend on the patient's tumor burden. If data on tumor burden were available, these could probably provide further explanation for the observed spread of whole-body doses. In most patients, however, tumor is usually widespread and disseminated throughout the body and the assessment of total tumor burden is not possible.

TABLE 2
Tumor Doses Obtained from Tracer Investigations and Whole-body Doses Absorbed during Therapy

Patient no.	Tumor dose (Gy/MBq)	Whole-body dose (mGy/MBq)	Therapeutic ratio (Tumor/Whole body)
1	16.9	0.13	130
2	5.2	0.16	32.5
3	4.1	0.11	37.3
4*	3.7	0.17	21.8
5	2.8	0.080	35.0
6	2.6	0.10	26.0
7	2.0	0.13	15.4
8	0.73	0.10	7.3
9	0.66	0.072	9.2
10	0.40	0.070	5.7

*Neuroblastoma patient; result from an earlier study, where tumor dose was calculated from combined pre- and post-therapy dosimetry. Others were pheochromocytoma patients.

Whole-body dose results are comparable with published data. Eartl et al. (*3*) calculated a mean whole-body dose of 0.11 mGy MBq^{-1} in a long-time retention study of three adult pheochromocytoma patients. Somewhat higher values were obtained in a study of 25 children with neuroblastoma aged between 1 and 10 yr, with a mean value of 0.33 ± 0.14 mGy MBq^{-1} (mean ± s.d.) (*23*). The low body weight of these patients, with similar clearance parameters T_1 and T_2, easily account for this difference.

Statistical Analysis

The tumor dose calculated in the diagnostic series was: D_T = 2.2 mGyMBq^{-1} (median value, range $0.4 \leq D_T \leq 20$ mGy MBq^{-1}). In the therapeutic series, the whole-body dose was: $D_{WB} = 0.12 \pm 0.04$ mGy MBq^{-1} (mean ± s.d. of 16 patients). Individual values, for the patients in whom therapy was complemented by quantitative diagnosis, are shown in Table 2 along with the corresponding therapeutic ratio value, calculated as $R = D_T/D_{WB}$ (tumor dose and whole-body dose were averaged for each patient). The therapeutic ratio varies from an extremely favorable value of 130 to an acceptable value of 20–30, to values below 10, which are probably too low to expect a positive outcome of the treatment. The values of tumor dose and whole-body dose are plotted in Figure 4. There is a proportionality between whole-body dose and tumor dose: increase in the latter results in the increase in the former.

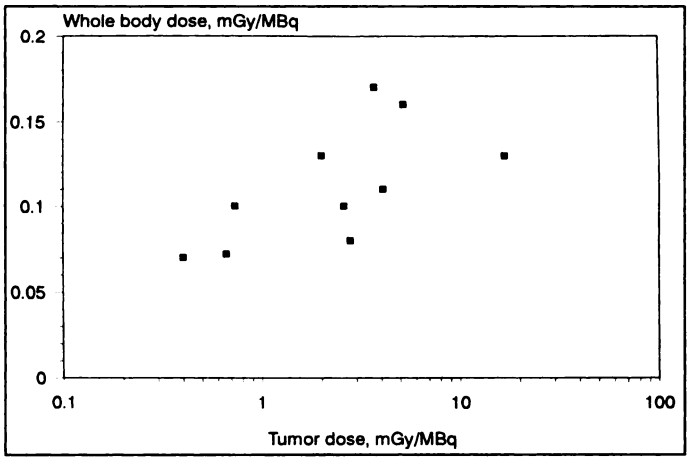

FIGURE 4. Whole-body dose versus tumor dose.

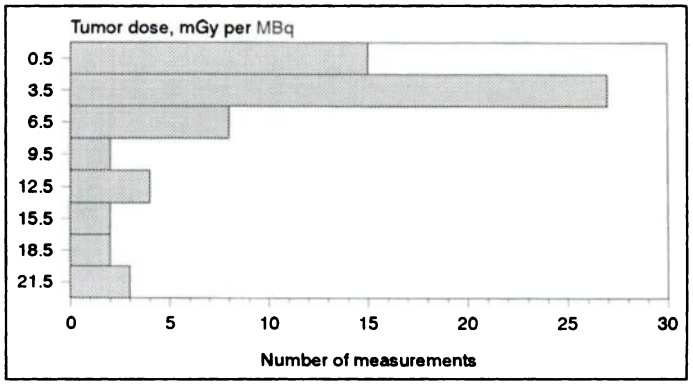

FIGURE 5. Summary of tumor dose distribution.

DISCUSSION

The values characterizing tumor uptake and retention are comparable with those quoted in the literature. In histopathological studies, Bomanji et al. (*24*) measured uptake of 0.01% per gram tissue in two pheochromocytomas at 22 hr and 0.13% per gram in another. Blake et al. (*25*) reported a biological half-life "between 1 and 2 days", using as an example a patient with a 30-hr value. Somewhat higher values were reported in the UKCCSG trial (Fielding, *personal communication,* 1989), with the mean uptake of 0.07% per gram tissue and mean half-life of 56 hr. This might be due to the nature of the tumors studied (i.e., neuroblastoma rather than pheochromocytoma). On the other hand, in an earlier study by Sisson et al. (*26*), high uptake (up to 0.18% per gram) in some pheochromocytomas was measured, with the corresponding half-life up to 72 hr. Similar results were reported later by the same group (*27*). Two small metastases, 2.6 cm^3 and 7 cm^3 volume, in a pheochromocytoma patient, showed extremely high uptake, 0.16 and 0.22% per gram, respectively, with corresponding half-lives of 50 and 70 hr. Another study of pheochromocytomas (*28*) reported modest values of uptake (between 0.01 and 0.05% per gram of tumor) but higher effective half-life values (40 to 200 hr). Rather than comparing uptake and effective half-life separately, a comparison of the tumor dose, which is proportional to both variables, gives a clearer picture.

The histogram in Figure 5 represents 63 measurements of tumor dose in pheochromocytoma: 27 are from results of the present study and the remainder from published data (*17,26,27,29*). Some of the results were obtained, as in the present work, from diagnostic studies, others from post-therapy quantification. The median value, D_T = 3.7 mGy MBq^{-1} (range $0.2 \leq D_T \leq 22.2$), is comparable with our result of 2.2 mGy MBq^{-1}. For the majority of measurements, the tumor dose is of the order of a few mGy per MBq; in exceptional cases, higher doses, in the order 10–20 mGy per MBq are estimated. In the present study, such exceptions have also been noted, in which the high tumor dose is the result of good uptake and prolonged retention. It is tempting to speculate that these patients stand the best chance of successful treatment. In other clinical studies, however, the correlation between the calculated absorbed radiation dose and tumor response remains poor (*22*). The patient who had the highest absorbed tumor dose measured in our series remains well 8 yr after the initial MIBG treatment. Because few patients receive really high tumor doses, reports of such cases are anecdotal. Perhaps this patient group deserves greater attention in future studies.

We calculated tumor doses from diagnostic investigations using tracer quantities of [^{123}I]MIBG and whole-body doses from treatments with therapeutic activities of [^{131}I]MIBG. The validity of the conclusions derived from the comparison of the

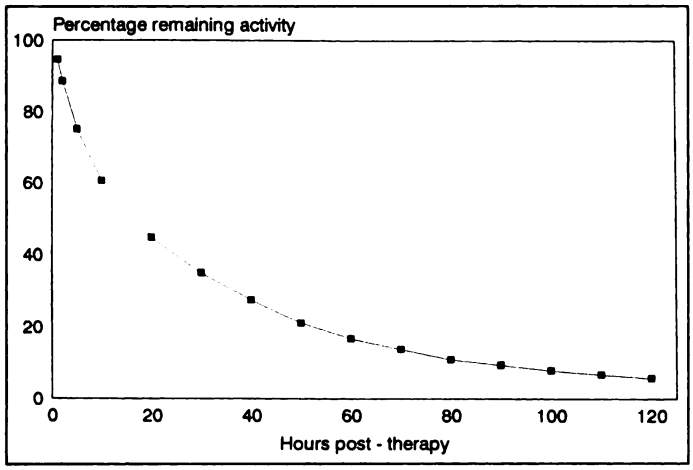

FIGURE 6. Composite retention curve for whole-body activity.

two series are valid depends on the accuracy of extrapolating diagnostic results to therapeutic results. Wafelman et al. (*22*) recently reviewed MIBG pharmacokinetics, cytotoxicity and dosimetry. They quote previous findings regarding the difference in biokinetics of tracer and therapy doses (i.e., accelerated clearance attributable to cell damage during therapy). It is not clear whether damaged tumor cells would account for such difference: Smets et al. (*30*) observed that uptake and retention in neuroblastoma and pheochromocytoma cell lines in culture were "minimally impaired by an externally delivered radiation dose of 5 Gy to mimic the radiobiological effect of [^{131}I]MIBG in tumors." The same authors, however, caution against uncritical extrapolation from low-dose diagnostic to high-dose therapy applications due to different concentration (the so-called "mass dose") of MIBG. They suggest that diagnostic studies probably overestimate the loading capacity of pheochromocytoma and certainly underestimate that of neuroblastoma. These comments, however, refer to a large (i.e., 30-fold) span in the range of concentrations. In the present study, patients received 2.5 mg MIBG in diagnostic investigations and 3.7–7.4 mg MIBG in the therapeutic studies: a maximum threefold difference. If concentration of MIBG does indeed affect uptake, the tumor dose during therapy would be somewhat smaller than that calculated in the diagnostic studies.

We combined all available retention data to produce a composite whole-body retention curve (Fig. 6). It can be conveniently described with a simple mathematical model, which assumes a continuous decline in clearance rate. The mean effective half-life increases from 5 hr at 1 hr postinjection to 35 and 45 hr at 3 and 5 days, respectively. The composite retention model is useful in radiation protection. It allows designation of controlled areas and estimation of permissible nursing and visiting times. At a distance of 1 m from the patient, the average dose rate after administration of 7.4 GBq [^{131}I]MIBG decreases from 300 μSvhr^{-1} immediately after injection to 120, 70 and 40 μSvhr^{-1} after 1, 2 and 3 days, respectively. By extrapolating the mean retention curve, predictions can be made for safe resumption of various activities. On average, patients can travel on private transport (800 MBq retained activity) after 3.5 days, on public transport (400 MBq) after 5 days, resume work, school and normal social contact (150 MBq) after 8 days and contact with children (30 MBq) 12 days after administration of 7.4 GBq MIBG. These values correspond to current United Kingdom regulations.

It is generally accepted that the most optimum effects are achieved when treatment with targeted radionuclides are pushed to toxic levels (*31*). There is, however, much less general

TABLE 3
Prescribed Administered Activity and Resulting Tumor Dose to Deliver 1 Gy Whole-body Dose

Patient no.	Administered activity (GBq)	Tumor dose (Gy)
1	7.7	130
2	6.3	32.5
3	9.1	37.3
4*	5.9	21.8
5	12.5	35.0
6	10.0	26.0
7	7.7	15.4
8	10.0	7.3
9	13.9	9.2
10	14.3	5.7

*Neuroblastoma patient, same as in Table 2.

agreement as to what exactly the limiting toxicity level should be. The 2.5-Gy whole-body dose (called $TD_{5/5}$, which causes minimal 5% complications in 5 yr, is derived from external beam radiotherapy using standard fractionation schedules) is too high, particularly if autologous bone marrow rescue cannot be relied upon and if repeated therapies are planned. With a 2.5-Gy whole-body dose, over 80% patients develop thrombocytopena; this percentage is reduced to 30% at 2.0 Gy. At 1.0 Gy, bone marrow suppression is rare (*23*). Therefore, a whole-body dose not much greater than 1.0 Gy appears to be a more appropriate limit if bone marrow transplantation is not part of the protocol and especially in patients whose bone marrow had been compromised as a result of previous chemotherapy, external beam radiotherapy or extensive bone marrow infiltration by tumor. Another limiting factor is of a practical nature: administered activities in excess of 11 GBq create significant radiation protection difficulties. Therapy doses usually range from 3.7 to 11 GBq, with recently reported results favoring rather higher doses (*32*).

We used the results on tumor and whole-body doses from those patients in whom both sets of data were available, to calculate the administered activities that would deliver a 1.0-Gy absorbed whole-body dose and the corresponding tumor dose (Table 3). Patient 1 would receive a high tumor dose from 7.7 GBq, which is close to the standard 7.4 GBq. In Patients 2–6, therapeutically useful tumor doses could be achieved with acceptable associated toxicity (in Patient 5, reducing activity to 11 GBq would give a tumor dose of 30.8 Gy). In Patient 7, tumor dose was lower, while in Patients 8–10, the administered activity and whole-body dose would have to be unacceptably high to achieve a tumor dose above 10 Gy (it is considered that lower doses have little chance to have a useful therapeutic effect). If doses during therapy were lower than those estimated from the diagnostic studies, even greater toxicity would have to be incurred to achieve efficacious tumor doses.

Dosimetry of systemically administered radionuclides is an integral part of patient management in the treatment of neuroectodermal tumors. The MIRD schema remains the accepted method of analysis for calculating absorbed doses to tumor and normal tissues. Its main problem is the assumption of homogeneous distribution of radiopharmaceutical in tissue. Tumors have a complex architecture and heterogeneous blood supply. This issue cannot be addressed within the MIRD framework, nor can the distinction be made between different ways in which radiopharmaceuticals localize in tissue (*27*). More ap-

propriate are the methods of cellular dosimetry, in which the dose to the nucleus, as the target of interest, is calculated.

CONCLUSION

We measured tumor and whole-body doses in patients diagnosed and treated with radioiodinated MIBG. The results generally corroborate those reported earlier. Comparisons with published data reveal that distribution of tumor doses is skewed, with very few patients receiving tumor doses in excess of 10 mGy/MBq of injected activity. At the other end of the spectrum, the delivery of a tumor dose below 1 mGy/MBq is unlikely to be beneficial. New results suggest that the use of no-carrier-added [^{131}I]MIBG might improve tumor targeting and therapeutic efficacy (*33*).

Radiosensitizers, such as carbogen and nicotinamide, could be used to overcome chronic and acute hypoxia of tumor cells, with a lower degree of sensitization in normal tissues (*34*). New strategies, combining the use of targeted radionuclide therapy with chemotherapy, surgery and external beam radiotherapy, are also undergoing clinical trials (*35*).

REFERENCES

1. Sisson JC, Shapiro B, Hutchinson RJ, et al. Predictors of toxicity in treating patients with neuroblastoma by radiolabeled metaiodobenzylguanidine. *Eur J Nucl Med* 1994;21:46–52.
2. Tytgat GAM, Voûte PA, Takeuchi S, Miyoshi I, Rutgers M. Metaiodobenzylguanidine uptake in platelets, megakaryoblastic leukaemia cell lines MKPL-1 and CHRF-288-11 and erythroleukaemic cell line HEL. *Eur J Cancer* 1995;31A:603–606.
3. Ertl S, Deckart H, Blottner A, Tautz M. Radiopharmacokinetics and radiation absorbed dose from ^{131}I-MIBG. *Nucl Med Commun* 1987;8:643–653.
4. Rubin P. The Franz Buschke Lecture: late effects of chemotherapy and radiation therapy: a new hypothesis. *Int J Radiat Oncol Biol Phys* 1984;10:5–34.
5. Wheldon TE, O'Donoghue JA. The radiobiology of targeted radiotherapy. *Int J Radiat Biol* 1990;58:1–21.
6. Alaamer AS, Fleming JS, Perring S. Evaluation of a technique for the quantification of radioactivity and volume of an object using SPECT. *Nucl Med Commun* 1993;14: 1061–1070.
7. Alaamer AS, Fleming JS, Perring S. Evaluation of the factors affecting the accuracy and precision of a technique for quantification of volume and activity in SPECT. *Nucl Med Commun* 1994;15:758–771.
8. Fleming JS. A technique for using CT images in attenuation correction and quantification in SPECT. *Nucl Med Commun* 1989;10:83–97.
9. Fleming JS. Technique for the use of standard outlines for attenuation correction and quantification in SPECT. *Nucl Med Commun* 1990;11:685–696.
10. McEwan AJ, Shapiro B, Sisson JC, Beierwalters WH, Ackery DM. Radio-iodobenzylguanidine for the scintigraphic location and therapy of adrenergic tumors. *Semin Nucl Med* 1985;15:132–153.
11. Shapiro B, Gross MD. Radiochemistry, biochemistry and kinetics of ^{131}I-MIBG and ^{123}I-MIBG: clinical implications of the use of ^{123}I-MIBG. *Med Pediatr Oncol* 1987;15:170–177.
12. Hoefnagel CA. Metaiodobenzylguanidine and somatostatin in oncology: role in the management of neural crest tumors. *Eur J Nucl Med* 1994;21:561–581.
13. Alaamer A. Quantification in single-photon emission computed tomography and its application to targeted radiotherapy and dosimetry. PhD thesis, University of Southampton; 1994.
14. Loevinger R, Budinger TF, Watson EE. MIRD primer for absorbed dose calculations. New York: The Society of Nuclear Medicine; 1988.
15. Snyder WS, Ford MR, Warner GG, Watson SB. "S" absorbed dose per unit cumulated activity for selected radionuclides and organs. *MIRD pamphlet No 11*. New York: The Society of Nuclear Medicine; 1975.
16. Hoefnagel CA. Radionuclide therapy revisited. *Eur J Nucl Med* 1991;18:408–431.
17. Fielding SL, Flower MA, Ackery D, Kemshead JT, Lashford LS, Lewis I. Dosimetry of iodine-131-metaiodobenzylguanidine for treatment of resistant neuroblastoma: results of a U.K. study. *Eur J Nucl Med* 1991;18:308–316.
18. Goddu SM, Howell RW, Rao DV. Cellular dosimetry: absorbed fractions for monoenergetic electron and alpha particle sources and S-values for radionuclides uniformly distributed in different cell compartments. *J Nucl Med* 1994;35:303–316.
19. Gaze MN, Mairs RJ, Boyack SM, Wheldon TE, Barrett A. Iodine-131-metaiodobenzylguanidine therapy in neuroblastoma spheroids of different sizes. *Br J Cancer* 1992;66:1048–1052.
20. Wheldon TE. Targeting radiation to tumors. *Int J Radiat Biol* 1994;65:109–116.
21. Amin AE, Wheldon TE, O'Donoghue JA, Barrett A. Radiobiological modeling of combined targeted ^{131}I therapy and total-body irradiation for treatment of disseminated tumors of differing radiosensitivity. *Int J Radiat Oncol Biol Phys* 1993;27:323–330.
22. Wafelman AR, Hoefnagel CA, Maes RAA, Beijnen JH. Radioiodinated metaiodobenzylguanidine: a review of its biodistribution and pharmacokinetics, drug interactions, cytotoxicity and dosimetry. *Eur J Nucl Med* 1994;21:545–559.
23. Lashford LS, Lewis IJ, Fielding SL, et al. Phase I/II study of iodine-131 metaiodobenzylguanidine in chemoresistant neuroblastoma: a United Kingdom children's cancer study group investigation. *J Clin Oncol* 1992;10:1889–1896.
24. Bomanji J, Levison DA, Flatman WD, et al. Uptake of iodine-123 MIBG by pheochromocytomas, paraganglioma and neuroblastomas: a histopathological comparison. *J Nucl Med* 1987;28:973–978.
25. Blake GM, Lewington VJ, Fleming JS, Zivanovic MA, Ackery DM. Modification by nifedipine of ^{131}I-metaiodobenzylguanidine kinetics in malignant phaeochromocytoma. *Eur J Nucl Med* 1988;14:345–348.
26. Sisson JC, Shapiro B, Beierwaltes WH, et al. Radiopharmaceutical treatment of malignant pheochromocytoma. *J Nucl Med* 1984;24:197–206.
27. Koral KF, Wang X, Sisson JC, et al. Calculation radiation absorbed dose for pheochromocytoma tumors in ^{131}I-MIBG therapy. *Int J Radiat Oncol Biol Phys* 1989;17:211–218.
28. Jacobsson L, Mattsson S, Johansson L, Lindberg S, Fjalling M. Biokinetics and dosimetry of ^{131}I-metaiodobenzylguanidine. *Proceedings of 4th Int Radiopharmaceutical Dosimetry Symposium.* Oak Ridge, Tennessee 1985;389–398.
29. Krempf M, Lumbroso R, Mornex AJ, et al. Use of *m*-[^{131}I]iodobenzylguanidine in the treatment of malignant pheochromocytoma. *J Clin Endocrinol Metab* 1990;72:455–461.
30. Smets LA, Janssen M, Rutgers M, Ritzen K, Buitenhuis C. Pharmacokinetics and intracellular distribution of the tumor-targeted radiopharmaceutical *m*-iodo-benzylguanidine in SK-N-SH neuroblastoma and PC-12 Pheochromocytoma cells. *Int J Cancer* 1991;48:609–615.
31. Sisson JC, Hutchinson RJ, Carey JE, et al. Toxicity from treatment of neuroblastoma with ^{131}I-metaiodobenzylguanidine. *Eur J Nucl Med* 1988;14:337–340.
32. Clarke SEM. Radionuclide therapy in oncology. *Cancer Treat Rev* 1994;20:51–71.
33. Mairs RJ, Russell J, Cunningham S, et al. Enhanced tumor uptake and in vitro radiotoxicity of no-carrier-added [^{131}I]metaiodobenzylguanidine: implications for the targeted radiotherapy of neuroblastoma. *Eur J Cancer* 1995;31A:576–581.
34. Pigott K, Dishe S, Saunders MI. Short communication: the addition of carbogen and nicotinamide to a palliative fractionation schedule for locally advanced breast cancer. *Br J Radiol* 1995;68:215–218.
35. Gaze MN, Wheldon TE, O'Donoghue JA, et al. Multi-modality megatherapy with [^{131}I]metaiodobenzylguanidine, high dose melphalan and total-body irradiation with bone marrow rescue: feasibility study of a new strategy for advanced neuroblastoma. *Eur J Cancer* 1995;31A:252–256.